

NUMERICAL SIMULATION OF MEANDERING OPEN CHANNEL FLOWS

Usman Ghani*, Naeem Ijaz* and Daulat Khan**

ABSTRACT

Flooding occurs worldwide and causes huge loss to human life and property. There is an ever increasing danger of floods due to global warming. The overbank flow studies are important for understanding flow behavior and bed shear stresses during floods and for devising flood protection strategies. This study is based on three dimensional numerical simulation of overbank flows in meandering channels. Four different flow cases were considered. The cases vary from each other in the sense of bed slope and overbank flow depth. There were two overbank flow depths for each bed slope. In this study a rectangular main channel flanked by floodplains on both sides has been considered. The simulation was carried out by solving 3D continuity and Reynolds averaged Navier Stokes equations using a finite volume based numerical code. The turbulence closure was achieved through standard $k - \epsilon$ turbulence model. A comparison of simulated primary depth averaged velocities and conveyance capacities of main channel with experimental results were made and good agreement was achieved. The simulations were also made for stream-wise velocities and secondary velocity vectors over different sections along the meander wavelength for the four cases to enhance the understanding of the primary and secondary flow fields and boundary shear stresses using numerical simulation. It was observed that the direction of secondary currents depends upon flow depth and their strength increases with increasing depth of flow. In compound channel flow cases, the overbank flow velocities are stronger than the inbank flow field. The bed shearing stresses at the apex of the meander were also found to have been under the influence of flow depth and secondary circulations. It was also established that standard $k - \epsilon$ turbulence model which is incapable of simulating straight channels flows can simulate meandering channels to good accuracy.

KEY WORDS: *Meandering channel, Computational fluid dynamics, Secondary flows, Mesh independence, $k - \epsilon$ turbulence model.*

INTRODUCTION

Compound meandering channel flows are the ones which occur in rivers during flooding. A complex flow mechanism exists in such flows and is under investigation for decades. Still a lot is to be done due to the complications involved in these types of flows. This is mainly due to the fact that water flow is three dimensional and is derived by the combined action of a number of factors including shear stresses, centrifugal forces, gravity forces and pressure driven forces. The momentum transfer at the main channel and floodplain interaction layers results in shearing stresses. River engineers are interested in two stage channel flows for developing river flood prediction techniques, for understanding the sediment movement and deposition process and for the planning of river and floodplain management. Due to these reasons compound channel flows are of much practical importance and engineering application. Flooding has much impact

on human lives and economy of the country. A number of ways are being explored for making research in floods. These include theoretical, laboratory or field observations and computational fluid dynamics (CFD) based techniques. Some researchers used sophisticated devices in field to study the flow behaviour¹.

The CFD is being used for the prediction of different river flow features since the last several years^{2,3}. As the numerical modelling is economical and quicker than the experimental techniques, therefore it is being used increasingly as compared to past. One of the most important problems in numerical modelling is the closure problem. To overcome this issue researchers are developing new turbulence models which are being tested and after detecting deficiencies either the existing models are modified or new models are made to overcome such deficiencies^{4,5}. There is no universal turbulence model which can be used with confidence in all the fluid flow scenarios.

* University of Engineering and Technology, Taxila, Pakistan

** Engineering, University of Engineering and Technology Peshawar

The simplest and most widely used turbulence model i.e. K-ε also has deficiencies and fails in a number of cases. For this reason, the testing of turbulence models in various aspects of meandering channel flows is also an ongoing research area. Some researchers investigated the presence of vegetation on flood plains and impact of geometric parameters in meandering channel flows^{6,7}. As stated above due to weak turbulent anisotropy driven secondary cells, - model can be tested for its suitability in meandering channel simulations. In the past some researchers used finite volume based 3D model SSIIM (Sediment Simulation In Intakes with Multiblock option)⁸ for this case. SSIIM uses the - turbulence model with a structured mesh.

The governing equations for open channel flow are continuity and Reynolds-averaged Navior-Stokes equations. For steady state incompressible flow, these equations can be written as:

Continuity equation

$$\frac{\partial U_i}{\partial x_i} = 0 \tag{1}$$

Momentum equation

$$U_j \frac{\partial}{\partial x_j} (U_i) = \frac{\nu}{\rho} \frac{\partial}{\partial x_j} \left(\frac{\partial U_i}{\partial x_j} + \frac{\partial U_j}{\partial x_i} \right) - \frac{1}{\rho} \frac{\partial P}{\partial x_i} + F_i + \overline{(-u_i u_j)} \tag{2}$$

Where *P* is the pressure, *ν* and *ρ* are the kinematic viscosity and density of the water, *U_i* is the time-averaged velocity component in *x_i* direc-

tion, *F_i* denotes external force, and *u_iu_j* are the Reynolds stresses which result from the decomposition of instantaneous velocities into their mean and fluctuating components.

In this study, a compound meandering channel with a rectangular cross section has been investigated. The model was first validated and then used for simulation purposes and for enhancing the understanding of primary and secondary flow behaviour at different critical locations of a meander wavelength. As the flow behavior changes considerably when the water goes over bank, therefore a systematic change in overbank flow depth was made and its impact on direction and strength of secondary cells at different sections along the meandering wavelength were investigated. Boundary shear stresses over the bed at the apex were also investigated. The ability of - model in simulating these types of flow was assumed from this numerical modeling.

EXPERIMENTAL DATA

A part of the work done by Martin Marriott at the University of Hertfordshire⁹ has been used for validation purposes. This experimental work was comprised of one planform. Two bed slopes with two overbank flow depths for each slope were employed in the experimentation. There were floodplains on both sides of the main meandering channel. The channel had a sinuosity of 1.3. The schematic diagram of the experimental channel used in this study is shown in Figure 1. Different experimental cases shown in this

Table-1: Different geometric parameters of the meandering channel

Main Channel	Rectangular	Crossover angle	70°
Top width B (m)	0.507	Centre line radius, r(m)	0.50
Bottom Width (m)	0.507	r/B	1.0
Depth, y (m)	0.115	Meander Length, L	1.880
Aspect Ratio, B ² /A	4.41	L/B	3.70
B/y	4.41	Floodplain Width	1.230
Sinuosity	1.30	Meander belt width	1.158

Table-2: Different hydraulic parameters used

Experimental referenc	Dischaerge (LS ⁻¹)	Total Depth (From water surface to channel bed, mm)	Flood plain Slope (mm)	Roughness
111	25.6	159	0.00142	0.414
112	33.8	185	0.00498	0.414
121	49.7	156	0.00175	0.274
122	78	192	0.00508	0.274

Table 3: Comparison of Observed and Calculated Results

Experinent Reference	Experimental water surface slope	Experimental Discharge at E (LS ⁻¹)	Calculated water surface slope	Calculated Discharge at E (LS ⁻¹)
111	0.00142	0.01695	0.00141	0.016734
112	0.00142	0.02043	0.00122	0.019774
121	0.00498	0.02894	0.0058	0.032415
122	0.00498	0.04454	0.0054	0.04379

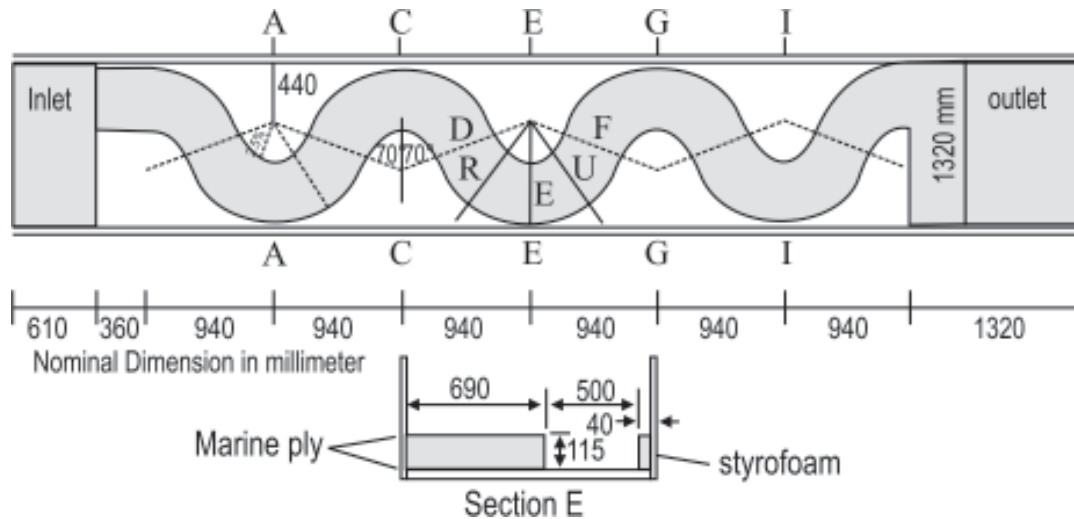


Figure 1: A schematic diagram of the channel used in the experimental work

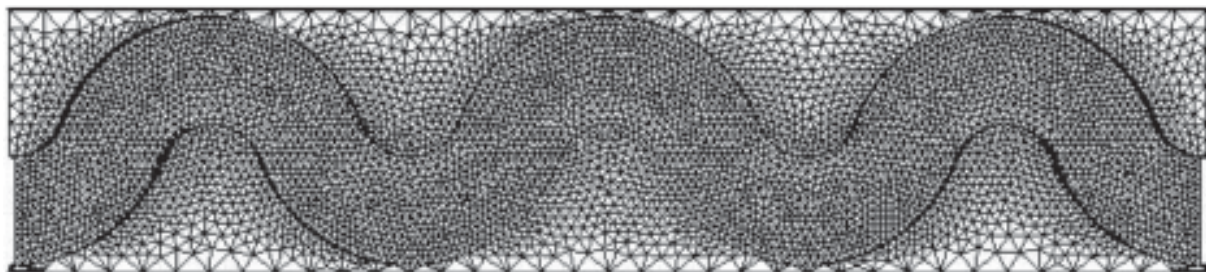


Figure 2: Unstructured mesh of the channel

paper have been named by three digits. These three digits represent geometry, slope (1 for low, 2 for high) and floodplain depth (1 for low and 2 for high) respectively. The experimental parameters employed in this numerical simulation have been shown in Table 1 and 2^{10,11}.

NUMERICAL MODEL

MODEL SETUP

This simulation work is based upon three dimensional continuity and momentum equations for open channel flows. These are time averaged (steady

state) incompressible flow equations. These are the fundamental equations for all the CFD based numerical codes as in the case of FLUENT¹².

The following boundary conditions were used in this study. A uniform velocity value was considered at the inlet whereas pressure outlet boundary condition was imposed at the exit of the flow domain. The side walls and bed were considered as no slip wall condition. A symmetry boundary condition was used at the free surface.

The convergence criteria was set as 1×10^{-6} . The under-relaxation coefficients were set at their default values as given in the FLUENT. The Semi-Implicit

Method for Pressure Linked Equations (SIMPLE) algorithm has been used for pressure-velocity coupling. The first-order upwind scheme has been incorporated for continuity, momentum, turbulence kinetic energy and its dissipation rate.

MESH GEOMETRY

The mesh generator available with FLUENT i.e. GAMBIT¹³ had been used for meshing purposes. The elements of the mesh were comprised of tetrahedral shapes. The node numbers in the streamwise, lateral and vertical directions of the main channel were 201×15×10 respectively. The mesh was dense close to the main channel boundaries where there were large velocity gradients. The mesh nodes on the floodplain were 36×15×6. For a check on mesh independence, the node numbers were doubled in x, y, and z directions. The unstructured mesh used in this study is shown in Figure 2.

RESULTS AND DISCUSSIONS

The results presented here are for five critical cross sections namely upstream cross-over (D), Apex (E), downstream cross-over (F), section between upstream cross-over and apex (R) and section between apex and downstream cross-over (U). All these sections have been shown in Figure 1. Primary velocities, secondary velocity vectors and discharge values have been simulated. Bed shear stresses have shown for the apex. The experimental data of an idealized laboratory meandering channel has been used for validation purposes. The numerical simulation results showed a close agreement between the calculated and observed water surface slope as shown in Table 3. Figure 3 (a-d) compares the calculated results of primary depth averaged velocities with observed ones. The convex side means inner edge and concave means outer edge of the meandering main channel. The results have been shown at the cross-overs, apex and two sections between apex and cross-overs. At the entrance of the bend (section D), a velocity dip phenomenon was observed towards the outer bank. This has been captured by the numerical calculations. At the beginning of the bend such as section R velocity values are higher towards the inner bank. It then gradually shifts towards the outer bank as is clear from the results of section F. All depth averaged velocity graphs indicated a good agreement between the observed and calculated values.

A shift of large momentum from inner bank of the main channel at the entrance (section D) towards outer bank at the exit (section F) has been observed both in observed and calculated results. The results at section F are a mirror image of those of section D as both are cross-overs one being at the upstream and the other at the downstream. Acceleration of primary velocity values at the inner bank has been observed while moving from upstream cross over to downstream cross over. Similar results have been observed in other three cases. Due to the non-availability of the observed average velocities at sections D and F, the comparison between simulated and observed ones could not be made for the case 112. The numerical results under predicted the velocity values for the case 122. However the trend of the observed and simulated velocity distributions was same.

Figure 4 (a to c) indicate the discharge calculations. From these diagrams it is clear that the simulated results gave a good agreement with the experimental ones for run 111. Although the simulated values are less than the observed ones but the maximum difference was 3.03% and 2.06% for discharges below the surface and below the floodplains respectively. The results showed that there is an increase in main channel discharge while moving from cross over towards the apex of the meander wavelength. However then there is a sudden decrease in the flow as the water moves downstream of the apex. At the downstream, both the secondary flows i.e. shear driven circulations from cross over and pressure driven from apex merge together. This combination of the two secondary circulations enhances the strength of secondary cells which flow from inner to outer bank of the main channel resulting in erosion of outer bank and expulsion of water from main channel to the floodplains. The same trend has been observed for cases 121 and 122.

Once the model capability established for meandering two stage channels, then the detailed primary and secondary velocity flow structure over different critical sections along the meander wavelength were explored. Figure 5 represents the predicted primary velocity contours overlaid by secondary velocity vectors. In these diagrams the ordinate represents the total height (depth) of flow from main channel bed to free surface. The negative values indicate in-bank flow depth while zero value represents the intersective values represent the water depth above the floodplain

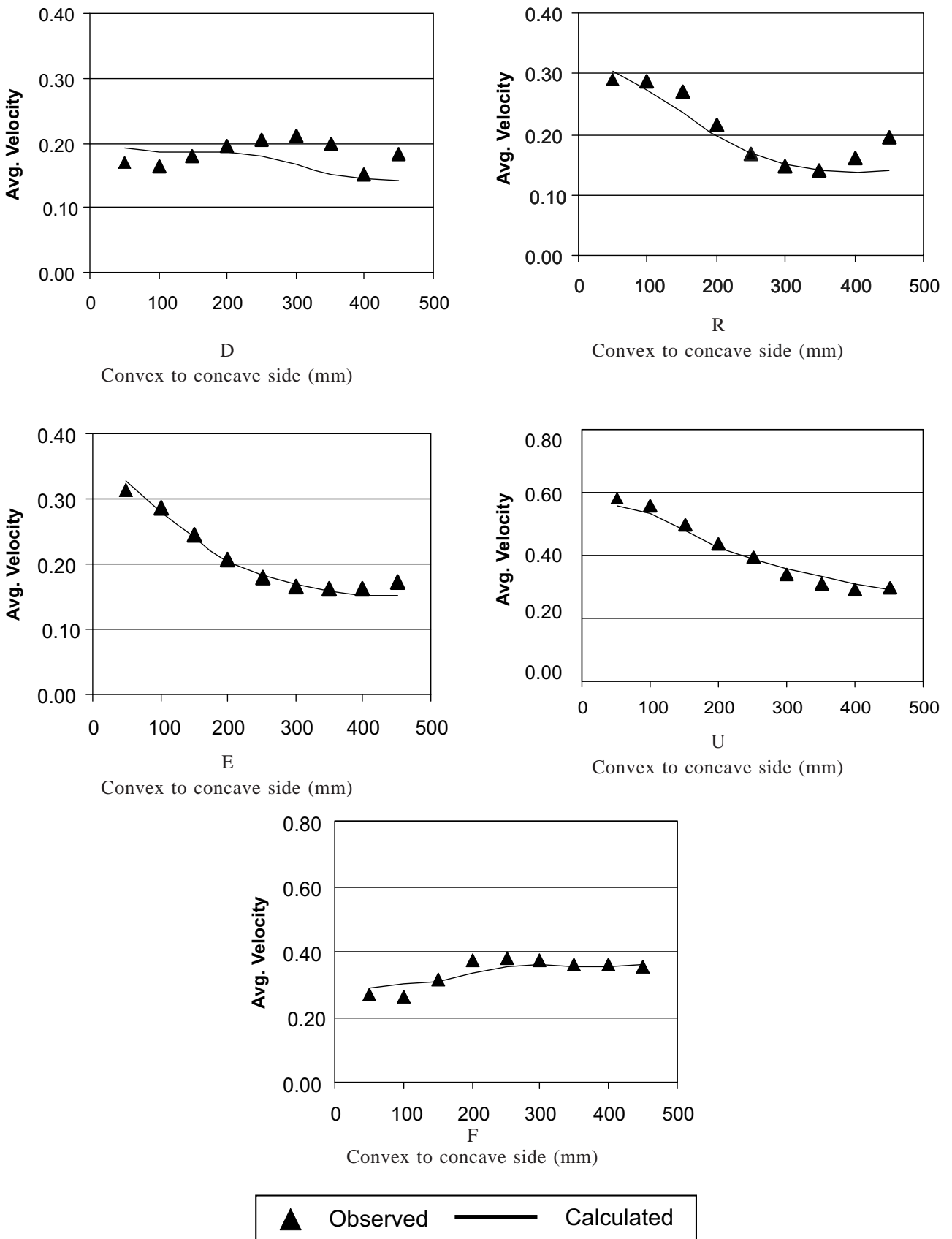


Figure 3(a)

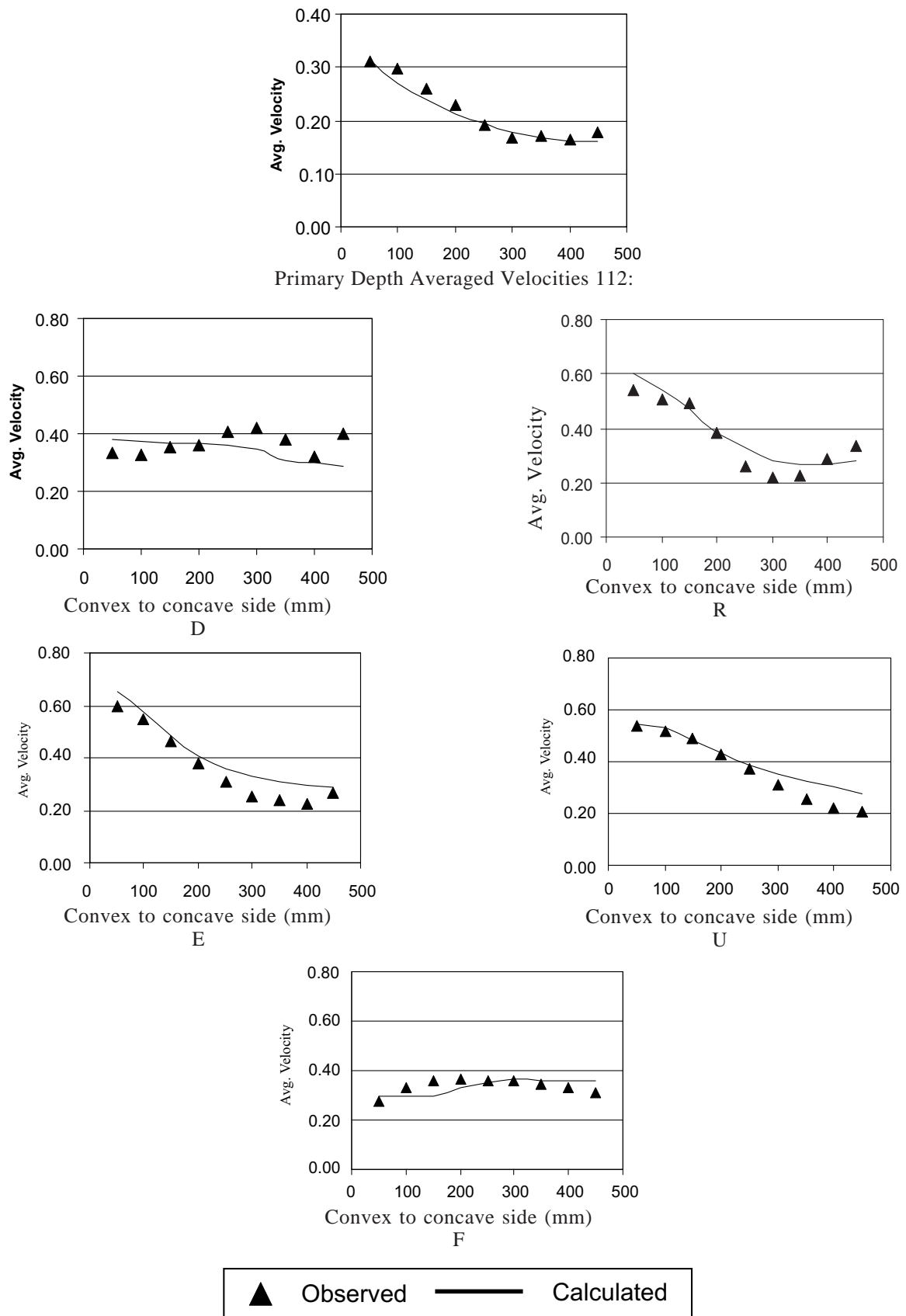
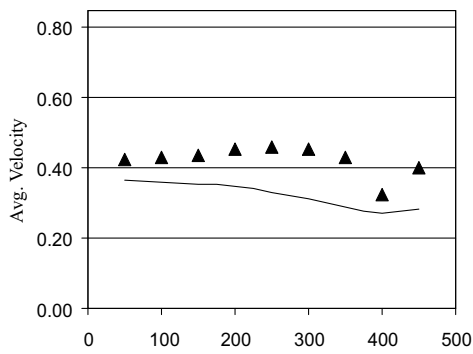


Fig. 3(c)



Primary Depth Averaged Velocities 122:

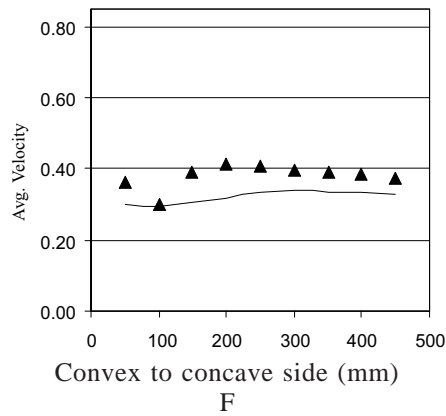
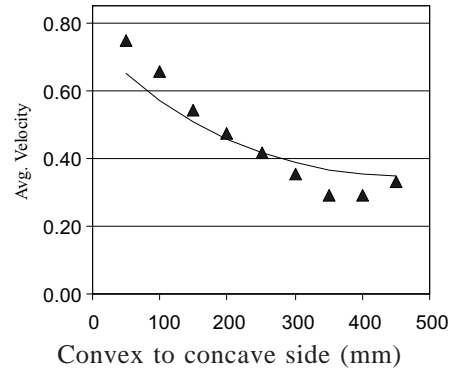


Fig. 3(d)

Comparison of Observed and Calculated Discharges:

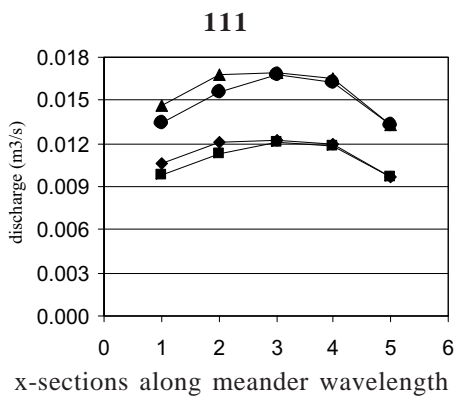


Fig. 4(a)

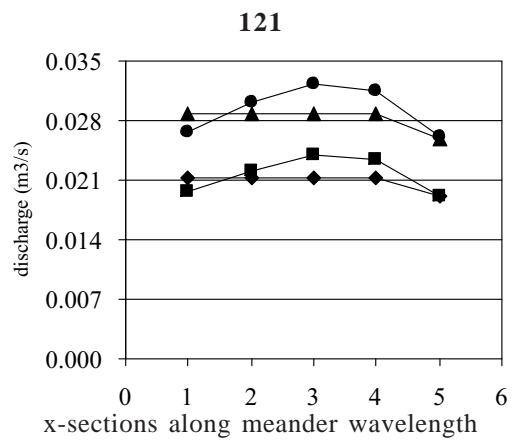


Fig. 4(b)

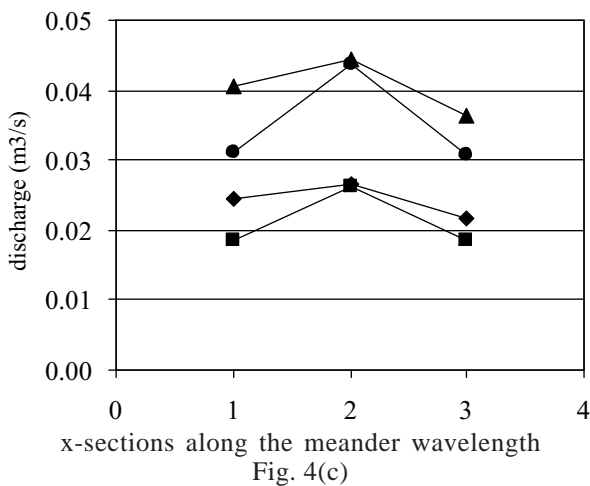
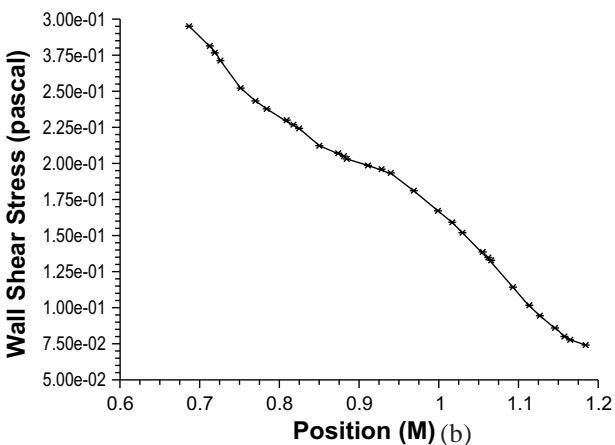
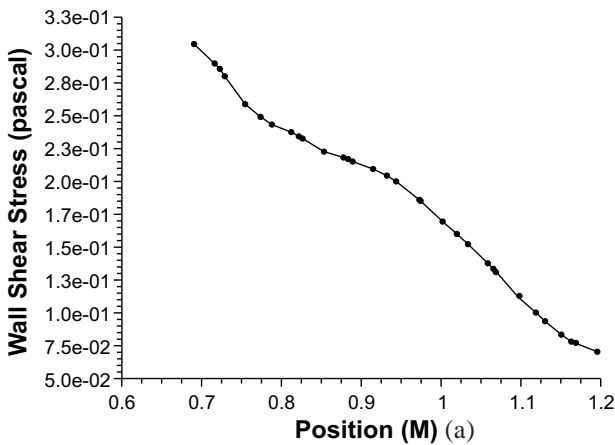
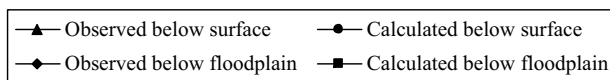


Fig. 4(c)



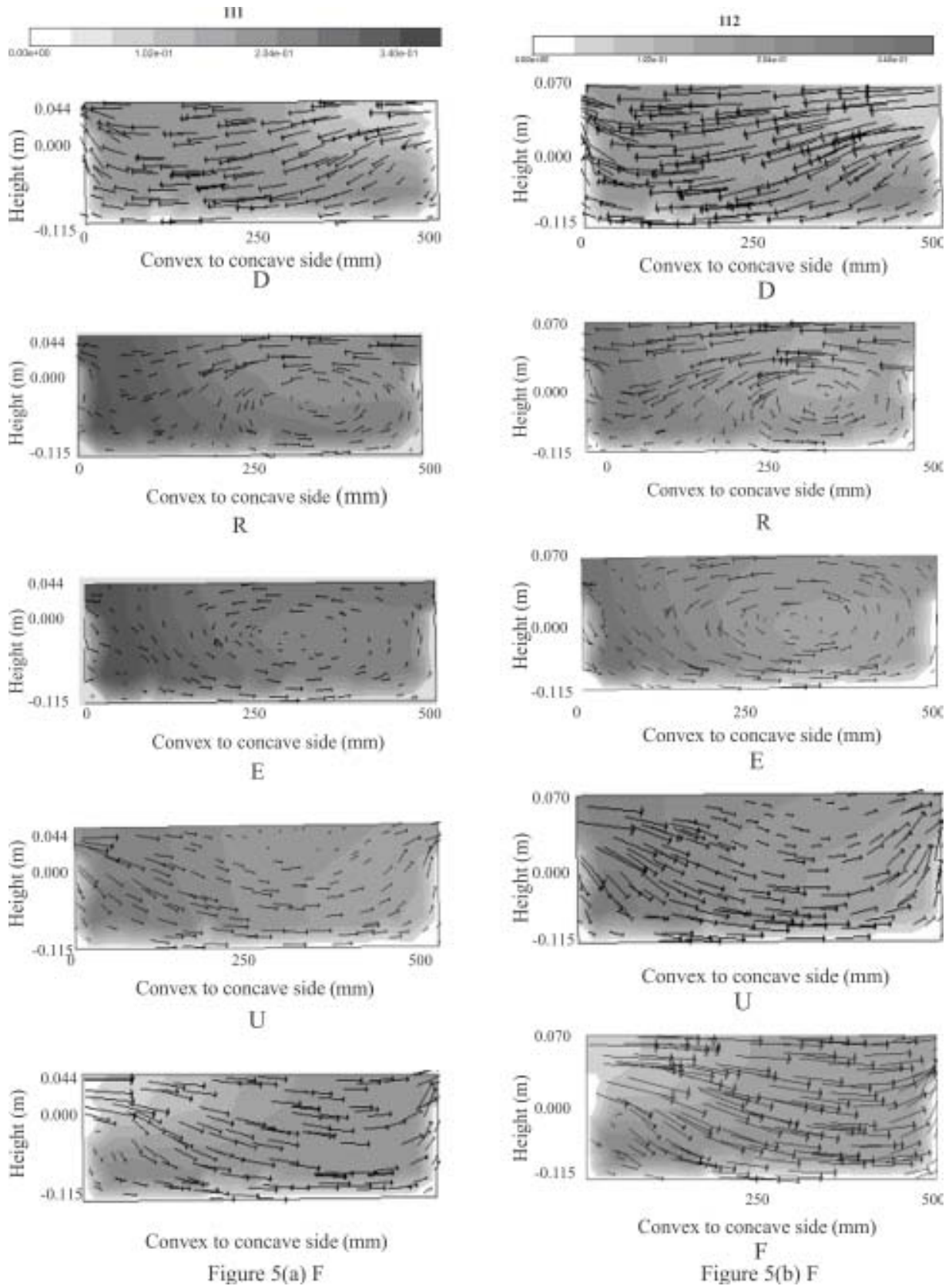
and main channel. The positive values represent the water depth. above the flood plain. It has been observed in Fig. 5(a) that close to the entrance of the bend (sections D and R) maximum primary velocity has happened near the inner bank and this occurred well below the free surface. As far as the secondary

currents are concerned, there intensity is more on the floodplain as compared to in-bank velocity magnitude. This might be attributed to the fact that within the main channel the entire section of channel offer resistance against flow i.e. more resistance has been offered by the boundaries of the channel while less resistance for flow is available over the floodplain. At the upstream cross-over the entire flow field is from outer to inner bank. The secondary flow field is quite strong over this section. Similar is the behaviour at the downstream cross over F. However at section R the velocity vectors close to the free surface are directed towards the inner bank while the velocity vectors close to the bed are moving towards the outer bank. As a result a counter-clockwise circulation was observed towards the outer bank. However the strength of these secondary vectors is less as compared to the section D. At section E which is the apex, a complete circulation has been observed but intensity has further reduced. After moving through the apex towards downstream sections, the secondary velocity vectors have again started gaining strength. This can be attributed to the existence of shear stress between the main channel flow and floodplain flow.

It has been observed that with increasing depth of flow, the strength of the secondary currents increases as is clear from a comparison of Figure 5 (a) and Figure 5 (b). Although the flow pattern is similar in both the cases but the intensity of secondary velocity vectors has considerably increased in the second case. In all these diagrams, upstream of the bend the direction of transverse flows is towards the inner bank which is opposite to in-bank flow situation. This might be attributed to the existence of centrifugal forces and the interaction between flows in the main channel and over the flood plains in two stage channels. Similar results were obtained in the cases where slope was changed i.e. cases 121 and 122 (Figure 5 c and d) where over bank flow depth also changed the intensity of the secondary velocity vectors.

Figure 6 (a) and (b) show the distribution of localized bed shearing stresses over the bed of the apex E for the cases 111 and 112. It was revealed that the wall shearing stresses had more intensity in the regions where secondary cells were directed towards the bed and less where the cells moved away from the bed. This can be attributed to the pushing force exerted by the secondary cells which increased the lo-

Figure 6: Distribution of localized bed shearing stress over the bed of the appexE for 111 and 112 Primary and Secondary velocities



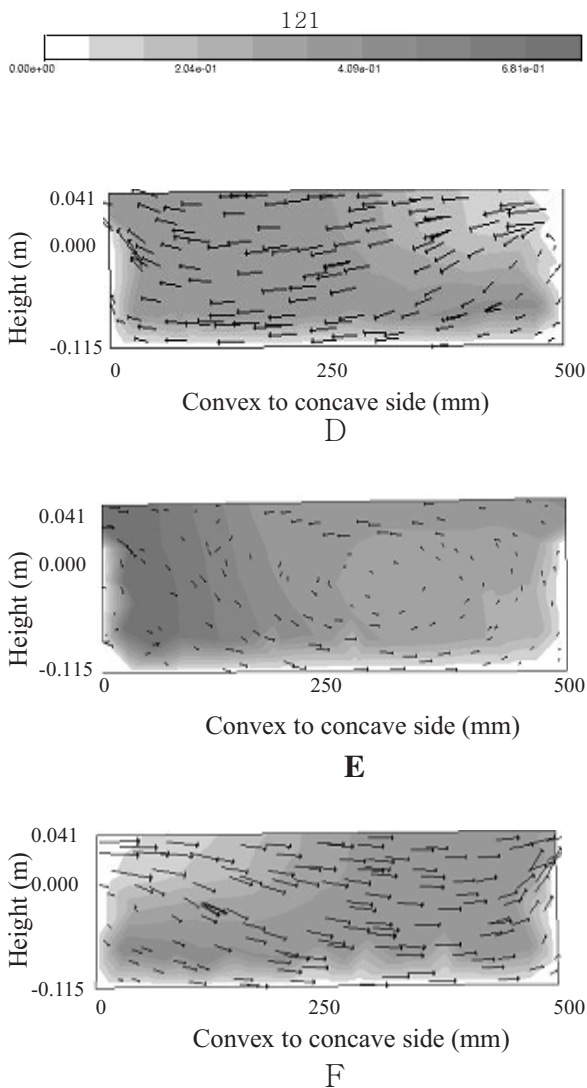


Figure 5(c)

calized bed shearing stresses. As far as the flow depth over the floodplain is concerned it had a mild (negligible) impact on the intensity of localized bed shearing stresses.

CONCLUSIONS

This study revealed that the direction of secondary currents depends upon flow depth above the floodplain. This has been observed in both cases of change of overbank flow depth i.e. when flow depth was increased from low overbank to high overbank, the secondary velocity cells gained strength. These results have been noticed in case of low as well as high bed slopes. In all the four flow situations, direction of transverse flows is towards the inner bank as the water enters the curvature. The results validated

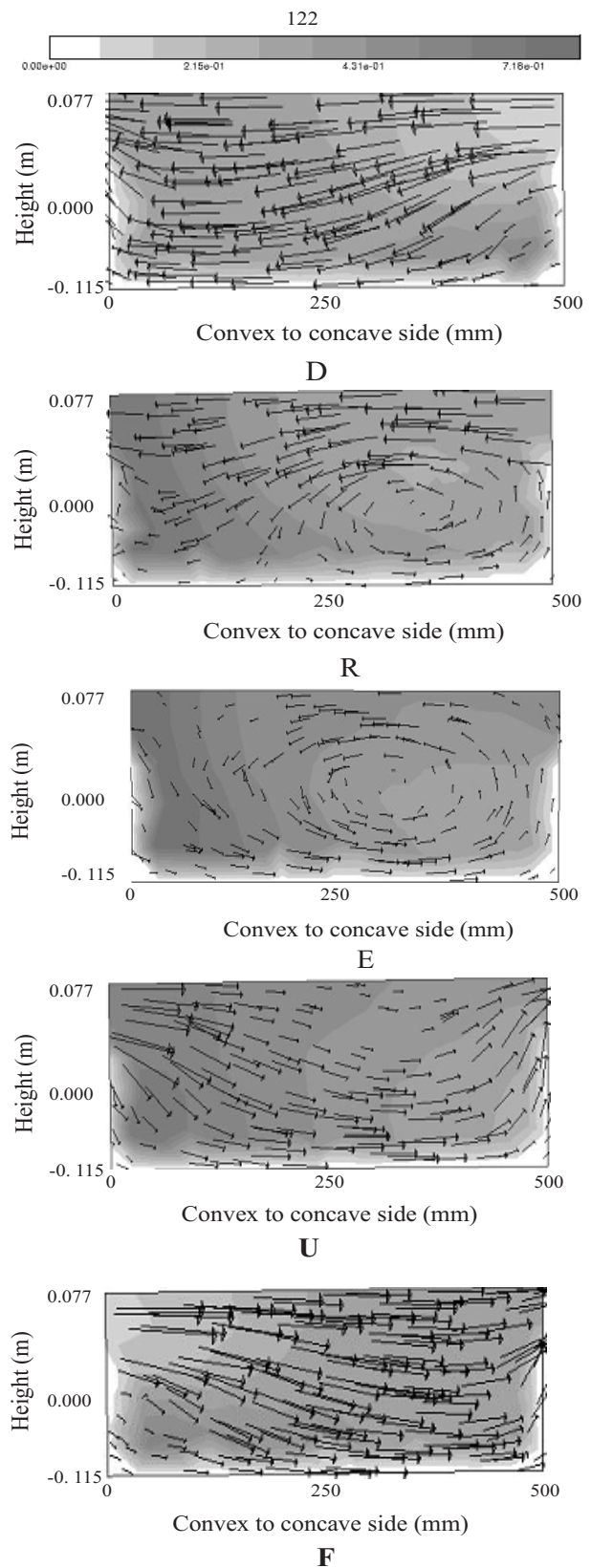


Fig. 5 (d)

Figure 5 (a → d): Secondary velocity vectors and primary isovels.

the presence of a velocity dip phenomenon at the entrance of the bend. This study revealed that the bed shearing stresses have more intensity in the region where secondary cells are directed towards the bed and less where the cells move away from the bed. Therefore in the outer regions of the apex, where the flow is directed upwards, the intensity of the bed shear stresses has reduced significantly. As far as the flow depth over the floodplain is concerned it has mild (negligible) impact on the intensity of localized bed shearing stresses. It also showed that although $k - \epsilon$ turbulence model is an isotropic turbulence model, even then it is suitable for overbank flow predictions in meandering channels. This can be attributed to the fact that the secondary cells in overbank flood flows are mainly dominated by centrifugal pressure variation at the apex and by the shear between main channel and floodplain flows. The side walls generated secondary cells are less dominant in these types of flows. Now both pressure and shear driven secondary flows are isotropic in nature, therefore the phenomena generated by them has been captured successfully by the isotropic turbulence model.

ACKNOWLEDGEMENT

The permission granted by Martin Marriott to use his data in this research is highly acknowledged.

REFERENCES

1. Jodeau M., Hauet A, Paquier A., Coz J, Dramaiz G, 2008. "Application and Evaluation of LS-PIV Technique for Monitoring of River Surface Velocities in High Flow Condition", *Journal of Flow Measurement and Instrumentation*, 19:117-127
2. Kang S, and Sotiropoulos F, 2012. "Numerical Modelling of 3D Turbulent Free Surface Flows in Natural Waterways", *Advances in Water Resources*, 40:23-36.
3. Antze F.T., Reuther N, Olson NRB, and Gutknecht D, 2009. "3D Modelling of Non-Uniform sediment Transport in a Channel Bend with Unsteady Flow". *Journal of Hydraulic Engineering*, 47:670-675.
4. Younis, B.A., 1996. "Progress in Turbulence Modelling for open Channel Flows, in *Fluvial Processes*", New York: Wiley.
5. Nezu, I., and Nakagawa, H. 1993. "Turbulence in open Channel Flows". Delft, Netherland: IAHR
6. Antze, T. F., 2001. "3D Numerical Modelling of open Channel Flows with Submerged Vegetation". *Journal of Hydraulic Research*, 39:303-310.
7. Marchis M.D. and Nepoli E., 2008. "The Effect of Geometric Parameters on the Discharge Capacity of Meandering Compound Channels". *Advances in Water Resources*. 31:1662-1673.
8. Olsen, N.R.B., 2004. "Sediment Simulation in Intakes Using Numerical Model-User Manual". Norway: The Norwegian University of Science and Technology.
9. Marriott, M. J., 1998. "Hydrodynamics of flow Around Bends in Meandering and Compound Channels", Ph.D. Thesis, University of Hertfordshire, UK,.
10. Marriott, M. J., "The Effect of Overbank flow on the Conveyance of the Inbank zone in Meandering Compound Channels". *IAHR Congress Graz Austria*. 28:1385-1394.
11. Wormleaton, P.R., and Marriott, M. J., 2007. "An Experimental and Numerical Study of the Effects of the Width of Meandering main Channel on Overbank Flows". *IAHR Congress Venice*, 36:670-680.
12. *User Guide Fluent 6.3*. Lebanon: FLUENT Incorporated Lebanon, New Hampshire, USA , 2005.
13. *User Guide Gambit 2.3*. Gnterra Resources Park 10 Cavendish Court, Lebanon: NH 03766.